

EXPLICIT PARAMETERIZATION OF EULER'S ELASTICA

PETER A. DJONDJOROV, MARIANA TS. HADZHILAZOVA[†],
IVAĬLO M. MLADENOV[†] and VASSIL M. VASSILEV

*Institute of Mechanics, Bulgarian Academy of Sciences
Acad. G. Bonchev Str., Bl. 4, 1113 Sofia, Bulgaria*

[†]*Institute of Biophysics, Bulgarian Academy of Sciences
Acad. G. Bonchev Str., Bl. 21, 1113 Sofia, Bulgaria*

Abstract. The consideration of some non-standard parametric Lagrangian leads to a fictitious dynamical system which turns out to be equivalent to the Euler problem for finding out all possible shapes of the lamina. Integrating the respective differential equations one arrives at novel explicit parameterizations of the Euler's elastica curves. The geometry of the inflexional elastica and especially that of the figure "eight" shape is studied in some detail and the close relationship between the elastica problem and mathematical pendulum is outlined.

1. Introduction

The elastic behaviour of rods and beams which attracts a continuous attention since the time of Galileo, Bernoulli and Euler has generated recently a renewed interest in plane [2, 3, 15], space [18] and space forms [1, 11]. The first elastic problem was posed by Galileo around 1638 who asked the question about the force required to break a beam set into a wall. James (or Jakob) Bernoulli raised in 1687 the question concerning the shape of the beam and had also succeeded in solving the case of the so called rectangular elastica (second case from the top in Fig. 1). Later on in 1742 Daniel Bernoulli wrote a letter to Euler in which he had suggested to him to solve the general problem of the elastica. Following closely this suggestion Euler cast the problem in the variational form and presented the solution in an Appendix to his book on variational calculus which appeared in 1744. Euler begins his investigation with establishing the equation of static equilibrium of the "lamina" by means of the variational techniques developed in his treatise and then rederives it from mechanical principles developed earlier by James Bernoulli. The

Bernoulli-Euler theory which considers only bending deformations and neglects shear deformations and stretching of the center line of the beam is given in detail by Love [13]. The corresponding solutions were found by using the equivalence of the elastica with that of the mathematical pendulum (see also Section five below).

Nine different classes can be distinguished and Love presents figures for the seventh of them (cf. Fig. 1 below). Later on Birkhoff and de Boor [2] have found the fundamental equation of the Euler elastica without length constraint (i.e., the so called free elastica)

$$\ddot{\kappa}(s) + \frac{1}{2}\kappa^3(s) = 0. \quad (1)$$

Here $\kappa(s)$ is the curvature of the arclength parameterized smooth curve in the plane and the dots denote the derivatives with respect to its natural parameter s .

In what follows we will derive the intrinsic equation of the non-free elastica by introducing a fictitious dynamical system and present its explicit solutions in terms of Jacobian elliptic functions and elliptic integrals.

We hope that these dynamical considerations could be of some interest in the many other situations as well.

2. The Fictitious Dynamical System

Assuming that λ is a positive real number let us consider the following system of nonlinearly coupled ordinary differential equations

$$\ddot{x} - \lambda z \dot{z} = 0 \quad (2)$$

$$\ddot{z} + \lambda z \dot{x} = 0. \quad (3)$$

It is quite natural to consider equations (2) and (3) as equations describing the dynamics of a particle moving in XOZ plane.

It is easy to check by a direct computation that equations (2) and (3) are the Euler-Lagrange equations

$$\frac{d}{ds} F_{\dot{x}} - F_x = 0, \quad \frac{d}{ds} F_{\dot{z}} - F_z = 0 \quad (4)$$

associated with an action functional whose Lagrangian F can be taken of the form

$$F(x, z, \dot{x}, \dot{z}, t) = \frac{1}{2} (\dot{x}^2 + \dot{z}^2) - \frac{\lambda}{3} z (z\dot{x} - x\dot{z})$$

in which λ plays the role of the Lagrange multiplier. The particle trajectories $\gamma(s) = \mathbf{x}(s)$ determined by the parametric equation

$$\mathbf{x}(s) = (x(s), z(s)) \quad (5)$$

which we will assume to be traced with unit speed, i.e.,

$$\dot{x}^2(s) + \dot{z}^2(s) = 1 \quad (6)$$

describe the plane curve we are seeking.

3. Integration

A theorem in the classical differential geometry (see e.g. [17]) claims that any plane curves is determined uniquely (up to Euclidean motion in the plane) by its curvature which in our settings can be written as

$$\kappa(s) = \dot{x}\ddot{z} - \dot{z}\ddot{x}. \tag{7}$$

It is easy to see also that the equations (2) and (3) imply

$$\kappa(s) = -\lambda z(s). \tag{8}$$

This claim can be proved in the following manner: multiplying (3) by \dot{x} and subtracting from it the result of multiplication of (2) by \dot{z} and taking into account (6) we get exactly (8)

$$\dot{x}\ddot{z} - \dot{z}\ddot{x} = -\lambda z.$$

Actually, the integration of (2) is immediate and produces

$$\dot{x} = \frac{\lambda z^2}{2} + \mu \tag{9}$$

where μ is the integration constant.

Inserting the expression for \dot{x} from (9) into (3) leads to the equation

$$\ddot{z} + \frac{\lambda^2 z^3}{2} + \lambda\mu z = 0. \tag{10}$$

When rewritten in terms of the curvature the above equation becomes

$$\ddot{\kappa}(s) + \frac{1}{2}\kappa^3(s) + \sigma\kappa(s) = 0, \quad \sigma = \lambda\mu \tag{11}$$

which is known as the intrinsic equation [3] of the elastica with tension σ and in this way we have reduced our fictitious dynamical system to the elastica problem.

Continuing with the integration of (10) we get

$$\dot{z}^2 = -\frac{\lambda^2 z^4}{4} - \lambda\mu z^2 + C \tag{12}$$

where C is another integration constant which however is not arbitrary but fixed by (6), i.e.,

$$C = 1 - \mu^2. \tag{13}$$

It is a trivial matter to find that the right hand side of equation (12) can be factorized in the form

$$\frac{\lambda^2}{4} \left(\frac{2(1-\mu)}{\lambda} - z^2 \right) \left(z^2 + \frac{2(1+\mu)}{\lambda} \right) \tag{14}$$

which allows the equation itself to be rewritten as

$$\int \frac{dz}{\sqrt{\left(\frac{2(1-\mu)}{\lambda} - z^2\right)\left(z^2 + \frac{2(1+\mu)}{\lambda}\right)}} = \frac{\lambda s}{2}. \tag{15}$$

Examination of the above integral leads to the conclusion that μ should be strictly smaller than one and further analysis shows that we have the following obvious possibilities:

- A) $\mu \in (-1, 1)$
- B) $\mu = -1$
- C) $\mu < -1$.

These possibilities will be considered below case by case:

a) Introducing

$$a^2 = \frac{2(1-\mu)}{\lambda}, \quad c^2 = \frac{2(1+\mu)}{\lambda}. \tag{16}$$

The integration in this case can be done with the help of the Jacobian elliptic function $\text{cn}(u, k)$ in which u is the argument and k is the so called modulus of the elliptic function (for more details on the elliptic functions, their integrals and properties see e.g. [7] and [10])

$$z(s) = a \text{cn}(-\sqrt{\lambda}s, k) = a \text{cn}(\sqrt{\lambda}s, k), \quad k = \sqrt{\frac{1-\mu}{2}} \tag{17}$$

b) The integration of the second case is performed via the hyperbolic functions and one easily gets

$$z(s) = \frac{2 \text{sech}(s\sqrt{\lambda})}{\sqrt{\lambda}}. \tag{18}$$

c) After some preparation the integration in the last case leads also to an expression in terms of Jacobian elliptic function. For that purpose we have to change the parameter μ with $\nu = -\mu$, which means that the range of the new parameter is the $\nu > 1$ part of the real line. Besides, it turns out convenient to introduce new parameters \hat{a} and \hat{c} in place of a and c used in (15), i.e.,

$$\hat{a}^2 = \frac{2(\nu+1)}{\lambda}, \quad \hat{c}^2 = \frac{2(\nu-1)}{\lambda} \tag{19}$$

so that this time we have to evaluate

$$\int \frac{dz}{\sqrt{(\hat{a}^2 - z^2)(z^2 - \hat{c}^2)}} = \frac{\lambda s}{2}. \tag{20}$$

Integrating it we obtain

$$z(s) = \hat{a} \text{dn}\left(-\sqrt{\frac{\lambda(\nu+1)}{2}}s, \hat{k}\right) = \hat{a} \text{dn}\left(\sqrt{\frac{\lambda(\nu+1)}{2}}s, \hat{k}\right), \quad \hat{k} = \sqrt{\frac{2}{\nu+1}}. \tag{21}$$

The above results should be completed by the integration of equation (9) in the appropriate setting and in this way we find respectively the parameterizations:

$$\begin{aligned}
 \text{A) } & x(s) = \frac{2}{\sqrt{\lambda}} E\left(\operatorname{am}\left(\sqrt{\lambda}s, k\right), k\right) - s, \quad z(s) = a \operatorname{cn}\left(\sqrt{\lambda}s, k\right) \\
 \text{B) } & x(s) = \frac{2 \tanh(\sqrt{\lambda}s)}{\sqrt{\lambda}} - s, \quad z(s) = \frac{2 \operatorname{sech}(\sqrt{\lambda}s)}{\sqrt{\lambda}} \\
 \text{C) } & x(s) = \hat{a} E\left(\operatorname{am}\left(\sqrt{\frac{\lambda(\nu+1)}{2}}s, \hat{k}\right), \hat{k}\right) - \nu s, \quad z(s) = \hat{a} \operatorname{dn}\left(\sqrt{\frac{\lambda(\nu+1)}{2}}s, \hat{k}\right)
 \end{aligned}
 \tag{22}$$

in which $E(u, k)$ and $F(u, k)$ (which will appear later on) denote the **incomplete elliptic integrals** of the **second** respectively **first kind** depending on the argument u and modulus k , and $\operatorname{am}(t, k)$ denotes the Jacobian amplitude function (cf. [7, 10]).

Actually, the integral (20) can be expressed in a slightly different form and this gives another curve

$$\begin{aligned}
 \text{C') } & x(s) = \hat{a} E\left(\operatorname{am}(u(s), \hat{k}), \hat{k}\right) - \frac{2\sqrt{2} \operatorname{cn}(u(s), \hat{k}) \operatorname{sn}(u(s), \hat{k})}{\sqrt{\lambda(\nu+1)} \operatorname{dn}(u(s), \hat{k})} - \nu s \\
 & z(s) = \frac{\hat{c}}{\operatorname{dn}(u(s), \hat{k})}, \quad u(s) = \sqrt{\frac{\lambda(\nu+1)}{2}}s
 \end{aligned}
 \tag{23}$$

which coincides with (22 C) (as it should be) if translated along the X axis at distance

$$\pm\sqrt{2} \left(\sqrt{\frac{\nu+1}{\lambda}} E\left(\operatorname{am}(K(\hat{k}), \hat{k}), \hat{k}\right) - \frac{\nu K(\hat{k})}{\sqrt{\lambda(\nu+1)}} \right)$$

where $K(\hat{k})$ is the **complete elliptic integral of the first kind** [7, 10].

4. Some Geometrical Remarks

A few comments are in order here. E.g., already Euler had detected nine species of elastic curves while in Fig. 1 we can see only seven of them. The remaining two, the straight line and the circle can be added immediately to the list. The first one is generated by the obvious solution $x(s) = s, z(s) \equiv 0$ of the governing system of equations (2) and (3). The circle respectively is the degenerated case of (22 C) when ν approaches infinity.

The rectangular elastica (second figure from the top in Fig. 1 is obtained when $\mu = 0$. Gibbons' [6] beautiful observation is that when this curve is rotated at $\pi/2$ it becomes the meridional profile of the Mylar balloon [14].

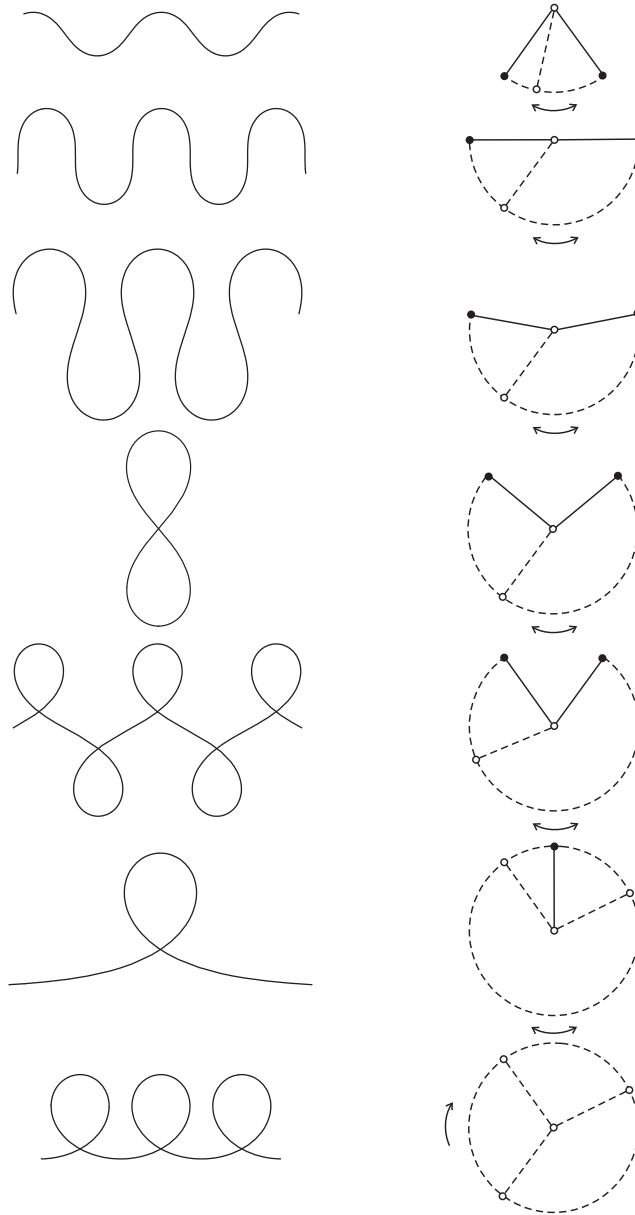


Figure 1. The elastic curves produced via formulas (22). In all cases the parameter λ is fixed, i.e., $\lambda = 4$. The first five figures starting from the top on the left hand side are generated by (22 A) and following values of μ : 0.5, 0, -0.4 , -0.65223 and -0.9 . The sixth one represents (22 B) while (22 C) in conjunction with $\nu = 1.2$ produces the last one.

Another interesting issue is how the value of μ producing the figure “eight” was found. To answer it let us make use of the fact that $\text{cn}(u, k)$ is periodic function of its argument u and its period is $4K(k)$.

Starting from the point A where $s = 0$ (see Fig. 2a) the elastic curve crosses for the first time the positive part of the OX axis for $\tilde{s} = K(k)/\sqrt{\lambda}$ at the point P which is $(2E(k) - K(k))/\sqrt{\lambda}$ off the origin O (here $E(k)$ denotes the **complete elliptic integral of the second kind**). In this setting it is clear that P will coincide with O provided we have arranged that

$$2E(k) - K(k) = 0. \tag{24}$$

This transcendental equation can be easily solved numerically by the modern computer algebra systems like Maple, *Mathematica*[®], Reduce, etc. In particular, the FindRoot command of *Mathematica*[®] produces

$$k = \sqrt{\frac{1 - \mu}{2}} \approx 0.908909 \tag{25}$$

and consequently

$$\mu = 1 - 2k^2 \approx -0.65223 := \hat{\mu}. \tag{26}$$

One can ask also the question how one can determine the aspect ratio, i.e.,

$$\eta = \frac{h_{\max}}{w_{\max}} \tag{27}$$

where h_{\max} and w_{\max} mean the maximal height, respectively width of the figure “eight”. According to the first item in (22) $h_{\max} = a$ specified in (16) and therefore we are left with the task to find w_{\max} . For that purpose we rewrite (9) and (12) in

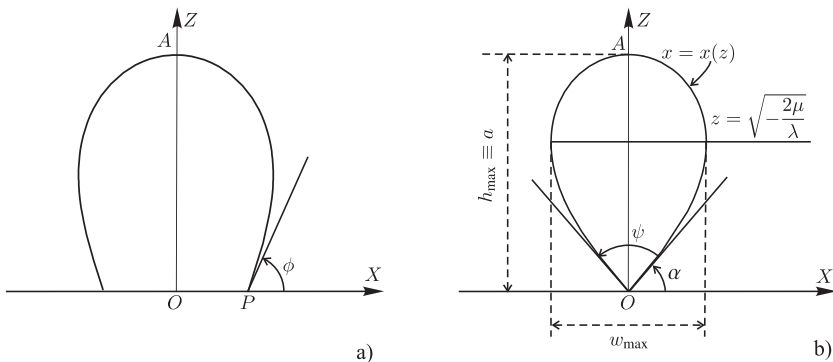


Figure 2. a) An elastic curve on the way to the figure “eight” shape. b) Geometry of the upper half of the figure “eight” elastica.

the form

$$\frac{dx}{dz} = \frac{z^2 + 2\mu/\lambda}{\sqrt{(a^2 - z^2)(z^2 + c^2)}} \quad (28)$$

from which is obvious that for $z < a$ after integration we will obtain a smooth function $x = x(z)$ describing the figure in the first quadrant. The entire figure can be built by the respective reflections from X and Z axes (see also Fig. 2b)).

Its maximal deflection x_{\max} from the Z axis is attained at the points where

$$\frac{dx}{dz} = 0. \quad (29)$$

Solving the last equation for z we obtain that the extremum takes place at

$$z = \sqrt{-\frac{2\mu}{\lambda}}. \quad (30)$$

Now, we have to determine the respective extremal value $x_{\max} = x(\sqrt{-2\mu/\lambda})$ but before that we have to integrate (28). Doing this we find

$$x(z) = \frac{1}{\sqrt{\lambda}} \left(2E(\arccos \frac{z}{a}, k) - F(\arccos \frac{z}{a}, k) \right) \quad (31)$$

and inserting (30) inside one finally gets

$$x_{\max} = \frac{1}{\sqrt{\lambda}} \left(2E(\arccos \sqrt{-\frac{\mu}{1-\mu}}, k) - F(\arccos \sqrt{-\frac{\mu}{1-\mu}}, k) \right). \quad (32)$$

Now, taking into account that $w_{\max} = 2x_{\max}$, we are in position to evaluate the aspect ratio as well, i.e.,

$$\eta(\mu) = \frac{\sqrt{1-\mu}}{\sqrt{2} \left(2E(\arccos \sqrt{-\frac{\mu}{1-\mu}}, \sqrt{\frac{1-\mu}{2}}) - F(\arccos \sqrt{-\frac{\mu}{1-\mu}}, \sqrt{\frac{1-\mu}{2}}) \right)} \quad (33)$$

which evaluated at $\mu = \mu^{\circ}$ produces with five digits precision

$$\eta(\mu^{\circ}) = 1.52408. \quad (34)$$

Evaluated at $\mu = 0$ corresponding to the rectangular elastica, or what is the same – the mylar balloon, formula (33) gives

$$\eta(0) = 0.834627 \quad (35)$$

a result which has been obtained in another settings in [14]. Let us notice also that by its very expression the aspect ratio is scale independent.

Our study of this class of solutions would be incomplete if we did not find the slope of the tangent to the elastica along the X axis. Fortunately, it is easy to conclude from (28) and Fig. 2 that

$$\cot \phi(\mu) = - \left. \frac{dx}{dz} \right|_{z=0} = - \frac{2\mu}{\lambda ac} = - \frac{\mu}{\sqrt{1-\mu^2}}. \quad (36)$$

At the origin which corresponds to $\mu = \hat{\mu}$ and where $\phi(\hat{\mu}) = \alpha$, the above formula gives $\cot \alpha = 0.860438$ and therefore $\alpha \approx 49.2901^\circ$. By the mirror symmetry this result tells us that the opening angle ψ of the figure “eight” is approximately 81.4199° (see Fig. 2b).

Another interesting geometric quantity which is also of some practical interest [16] is the area bounded by the elastica curves and the X axis. In Fig. 3 we have presented various such instances depending on the chosen values of μ .

For the area \mathcal{A} of any of the striped regions there we can write

$$\mathcal{A} = \int z dx = \int z \frac{dz}{dz} dz = \int \frac{z^3 + 2\mu z/\lambda}{\sqrt{(a^2 - z^2)(z^2 + c^2)}} dz. \tag{37}$$

For the solutions of class A) $z(s) = a \operatorname{cn}(\sqrt{\lambda}s, k)$, the problem with evaluation of the last integral reduces to the computations of the integrals of the first and the third powers of the Jacobian elliptic function cn which are tabulated (see [4]) and we have respectively

$$\begin{aligned} \int \operatorname{cn}(u, k) du &= \frac{1}{k} \arcsin(k \operatorname{sn}(u, k)) \\ \int \operatorname{cn}^3(u, k) du &= \frac{1}{2k^3} [(2k^2 - 1) \arcsin(k \operatorname{sn}(u, k)) + k \operatorname{sn}(u, k) \operatorname{dn}(u, k)]. \end{aligned} \tag{38}$$

With the help of the formulas listed above and taking into account the limits of the integration we find immediately that

$$\begin{aligned} \int \frac{z dz}{\sqrt{(a^2 - z^2)(z^2 + c^2)}} &= \arcsin(k) \\ \int \frac{z^3 dz}{\sqrt{(a^2 - z^2)(z^2 + c^2)}} &= \frac{\sqrt{1 - \mu^2}}{\lambda} - \frac{2\mu}{\lambda} \arcsin(k). \end{aligned} \tag{39}$$

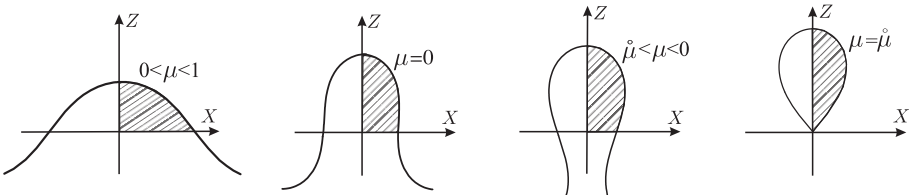


Figure 3. The striped regions present half of the area enclosed by the respective elastica curve and the X axis.

These combined results give at the end the amazingly simple formula for the total area $\mathcal{A}_{\text{tot}} = 2\mathcal{A}$ enclosed by the elastica and the X axis, i.e.,

$$\mathcal{A}_{\text{tot}} = \frac{2\sqrt{1-\mu^2}}{\lambda} = \sqrt{\frac{1+\mu}{1-\mu}} a^2 = \frac{4k\tilde{k}}{\lambda} = \frac{\tilde{k}}{k} a^2 \tag{40}$$

where \tilde{k} is the so called complementary elliptic modulus defined by the equation

$$\tilde{k}^2 = 1 - k^2. \tag{41}$$

In particular, for the rectangular elastica (the mylar balloon) we have $\mu = 0$, which implies $k = \tilde{k} = \frac{1}{\sqrt{2}}$ and therefore $\mathcal{A}_{\text{tot}} = a^2$.

5. Mechanical Aspects

Finally, we will add a few comments on the dynamical aspects of the elastica. Looking at Fig. 4 where $\theta(s)$ denotes the angle between the normal vector to the curve and the Z axis one easily concludes that

$$\dot{x}(s) = \cos \theta(s), \quad \dot{z}(s) = -\sin \theta(s) \tag{42}$$

and therefore

$$\dot{\theta}(s) = -\lambda z(s). \tag{43}$$

Differentiating once more the above equation we obtain just the equation of the mathematical pendulum (with negative string constant)

$$\ddot{\theta}(s) = \lambda \sin \theta(s) \tag{44}$$

and in this way we have established the close relationship which exists between this fundamental mechanical system and the Euler’s elastica.

This situation is depicted graphically in Fig. 1 where on the left hand side are shown various types of elastica configurations and on the right hand side the corresponding pendulum motions. The inflexional elastica corresponds to oscillatory motion of the pendulum, the single-looped elastica corresponds to the limiting case when its motion starts close to the position of unstable equilibrium at the top of the

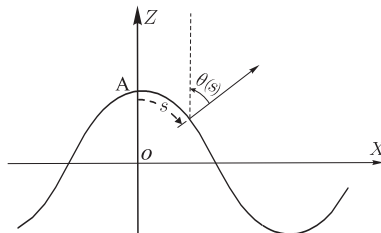


Figure 4. Geometry of the elastic curve in terms of the azimuthal angle $\theta(s)$.

circle and makes just one complete revolution, and the non-inflexional elastica corresponds to the revolving pendulum.

In the particular case most studied here when the pendulum furnishes oscillations corresponding to figure “eight” elastica the bob rises just to angle $\psi/2 \approx 40.71^\circ$ over the horizon. There remains, however the question about the mechanical interpretation of the figure “eight” for the pendulum motion.

It should be mentioned also that another set of explicit formulas describing the elastica's shapes can be found in the book by Love [13] who had derived them by integrating (44) directly.

Let us end with a remark that the Bernoulli-Euler beam equation is still a subject of real interest in view of its importance for analysis of large-deflection mechanisms as evidenced in [8, 9, 12] or its potential applications to nanotechnology or textiles problems [5].

6. Acknowledgments

This research is partially supported by the Bulgarian Science Foundation under a grant B-1531/2005 and a contract # 23/2006 between the Bulgarian and Polish Academies of Sciences. The authors are quite grateful to Professor Clementina Mladenova from the Institute of Mechanics, Bulgarian Academy of Sciences, for providing an access to her computer and computer algebra system *Mathematica*[®] via which some of the calculations presented here were done.

One of the authors (IM) would like to express his sincere thanks to many colleagues around the world, and among them Professors Carl de Boor (Wisconsin University), Oscar Garay (Bilbao University), Guido Brunnert (Technische Universität Chemnitz), Antoni Colom (Universitat de les Illes Balears), Ivan Dimitrov (Queens University), Velimir Djurdjevic (Toronto University), Garry Gibbons (Cambridge University), Larry Howell (Brigham Young University), Osman Kopmaz (Uludag University), David Mumford (Brown University) and Daniele Ritelli (Bologna) who kindly provide not only the reprints of their own works but in many cases also copies of other important papers on the fascinating subject of elastica.

References

- [1] Arroyo J., Garay O. and Menciá J., *Extremals of Curvature Energy Actions on Spherical Closed Curves*, *J. Geom. Phys.* **51** (2004) 101-125.
- [2] Birkhoff G. and de Boor C., *Piecewise Polynomial Interpolation and Approximations*, In: Proc. General Motors Symposium of 1964, H. Garbedian (Ed), Elsevier, Amsterdam, 1965 pp. 164-190.

- [3] Brunnert G., *A New Characterization of Plane Elastica*, In: *Mathematical Methods in Computer Aided Geometric Design II*, T. Lyche and L. Schumaker (Eds), Academic Press, New York, 1992 pp. 43–56.
- [4] Byrd P. and Friedman M., *Handbook of Elliptic Integrals for Engineers and Scientists*, Springer, Berlin, 1971.
- [5] Colom A., *Analysis of the Shape of a Sheet of Paper When Two Opposite Edges Are Joined*, *Am. J. Phys.* **74** (2006) 633–637.
- [6] Gibbons G., *The Shape of a Mylar Balloon as an Elastica of Revolution*, DAMTP Preprint, Cambridge University, 2006, 7pp.
- [7] Gradshteyn I. and Ryzhik I., *Tables of Integrals, Series and Products*, Academic Press, New York, 1980.
- [8] Hasan M. and Lilov L., *Closed-Form Solution for Large-Deflection Beams in Compliant Mechanisms*, *JTAM (Sofia)* **36** (2006) 27–42.
- [9] Howell L. and Midha A., *Parametric Deflection Approximation for End-Loaded Large-Deflection Beams in Compliant Mechanisms*, *ASME J. Mech. Design* **117** (1995) 156–165.
- [10] Jahnke E., Emde F. and Lösch F., *Tafeln Höherer Funktionen*, Teubner, Stuttgart, 1960.
- [11] Jurdjevic V., *Geometric Control Theory*, Cambridge University Press, Cambridge, 1997.
- [12] Kopmaz O., *On the Curvature of an Euler-Bernoulli Beam*, *Int J Mech Eng Edu* **31** (2003) 132–142.
- [13] Love A., *The Mathematical Theory of Elasticity*, Dover, New York, 1944.
- [14] Mladenov I. and Oprea J., *The Mylar Balloon Revisited*, *Am. Math. Monthly* **110** (2003) 761–784.
- [15] Mumford D., *Elastica and Computer Vision*, In: *Algebraic Geometry and Its Applications*, C. Bajaj (Ed), Springer, Berlin, 1994 pp 491–506.
- [16] Newman B., *Shape of a Towed Boom of Logs*, *Proc. R. Soc. Lond. A* **346** (1976) 329–348.
- [17] Oprea J., *Differential Geometry and Its Applications*, Second Edition, Prentice Hall, New Jersey, 2003.
- [18] Scarpello G. and Ritelli D., *Elliptic Integral Solutions of Spatial Elastica of a Thin Straight Rod Bent Under Concentrated Terminal Forces*, *Meccanica* **41** (2006) 519–527.